Elastic properties of bismuth borate glasses

Elastic properties of bismuth borate glasses

A El-Adawy†§ and Y Moustafa‡

† Physics Department, Faculty of Science, Monoufia University, Egypt
‡ Physics Department, Faculty of Science, Mansora University, Egypt

Abstract. The elastic properties of the vitreous system Bi_2O_3–B_2O_3 have been measured by ultrasonic pulse echo overlap technique at a frequency of 10 MH_z and at room temperature. For the purpose of measuring the ultrasonic velocity with high accuracy, the McSkimin criterion for determining the correct cyclic overlap between echoes is used. The elastic properties of the present glass system as a function of composition are discussed on the basis of the elastic internal energy due to the deformation. Also presented is a full discussion of the Poisson's ratio; which is found to be rather sensitive to the glass composition.

1. Introduction

Interest in glasses has rapidly increased in recent years because of diverse applications in electronics, nuclear and solar energy technologies and acousto-optic devices. Vitreous boron oxide, a well known oxide glass, has been studied since the early 1930s [1–4]. Pure boron oxide is a very good former, covalently bonded, with interesting physico-chemical properties. B_2O_3 and related binary borate systems (especially alkali borate glasses) are also of commercial and technological interest [1, 5].

The propagation of ultrasonic waves in solids provides important information regarding solid-state motion in the materials. Two types of acoustic waves are important [6]: bulk acoustic waves and acoustic surface waves. For basic studies in solids, bulk acoustic waves are mainly used, whereas for device applications, acoustic surface waves may be more appropriate. The propagation of acoustic waves in bulk glasses has therefore been of considerable interest in understanding mechanical behaviour.

The network structure and elastic properties of borophosphate glasses have been studied in terms of the fractions of four coordinated boron atoms, Osaka *et al* [7]. The elastic moduli of alkaline earth borate glasses was studied by Kodoma [8]. Paul *et al* [9] studied the ultrasonic velocity, absorption and elastic properties of barium borate glasses. They observed velocity dispersion with frequency and temperature. The elastic moduli of these glasses were calculated theoretically, assuming the Makishima and Mackenzie's model [9, 10]. No particular trend was observed in the ultrasonic velocity at a given frequency for these glasses [9]. The acoustic velocity in several glasses in the temperature range 73–473 K was measured by Fuxi *et al* [11]. The relationship between the structure and properties or the glasses and changes in the coordination number of

individual glass-forming cations in alkali oxide glasses have been analysed. The ultrasonic velocity and attenuation measurements in borate glasses at different temperatures were reported by Yawale *et al* [12, 13] and Pakade *et al* [14]. Nagate *et al* [15] measured the ultrasonic velocity and absorption in sodium borate and lead borate glasses at different temperatures. They suggested the the product of one-third power of the velocity of sound and the molar volume of the oxide melt was constant and independent of temperature.

In this work, the ultrasonic velocity, measured with high accuracy using the pulse echo overlap method [16], and the elastic properties as a function of composition, on the basis of the elastic internal energy due to the deformation of the bismuth borate glasses, are reported.

2. Theoretical considerations

The finite elastic strain theory [17, 18], in which the strain does not need to be infinitesimal, gives a complete description of the thermodynamic potentials, with stress and strain as the mechanical variables. In considering a deformed body at some temperature, we chose the undeformed state to be the state of the body at the same temperature in the absence of external forces. Let a_i, $i = 1, 2, 3$, denote the Cartesian coordinates of a material's particle before the deformation and $\lambda_i(a_1, a_2, a_3)$ denote the coordinates of the same particle after the deformation. Then the Lagrangian strain components η_{ij} which describe the finite elastic strains are given by

$$\eta_{ij} = \frac{1}{2}\left(\frac{\partial \lambda_k}{\partial a_i}\frac{\partial \lambda_k}{\partial a_i} - \delta_{ij}\right) \tag{1}$$

where i, $j = 1, 2, 3$ and the symbol δ_{ij} is the Kronecker delta.

Instead of the tensor notation, we use the abbreviated Voigt notation and the Lagrangian strain in the abbreviated

§ Present address: Sultanate of Oman, Sohar, PO Box 135/311.

notation is defined by Brugger [18] as

$$\eta_\alpha = 2\eta_{ij}/(1 + \delta_{ij}).$$

Because the sound wave propagates under adiabatic conditions, the internal energy is chosen in the present work as the most convenient thermodynamic potential. Let u and s be the internal energy and the entropy respectively, taken per unit mass; U and S taken per unit volume; and U_m and S_m taken per unit mole. Then, for the energy equation for conservative media [18], the internal energies can be expressed by

$$du = T\,ds + (1/\rho)t_\alpha\,d\eta_\alpha \qquad (2a)$$

$$dU = T\,dS + t_\alpha\,d\eta_\alpha \qquad (2b)$$

$$dU_m = T\,dS_m + (M/\rho)t_\alpha\,d\eta_\alpha \qquad (2c)$$

where T is the temperature, ρ is the density of the undeformed state, M is the molar mass, $t_\alpha = \rho(\partial u/\partial \eta_\alpha)_s$ is a quantity called the thermodynamic tension, and the summation is taken over the suffix α from one to six. Equations (2a) and (2b) are the usual expressions when the composition change is not to be considered, while (2c) is the new expression suitable for discussing elastic properties as a function of composition. These are the fundamental thermodynamic relations for the internal energies of a deformed body.

In order to be able to apply the general formulae of the internal energy to any particular deformation, we must know the internal energy of the body as a function of the strain. This expression is easily obtained by using the fact that the deformation is small and by expanding the internal energy in powers of η_α. As the glass is elastically isotropic, we shall consider here only isotropic bodies. Since $t_\alpha = 0$ when no external stresses are present, it follows that there are no first-order terms in the expansions of the internal energy in powers of η_α. The second derivatives of the internal energy with respect to the Lagrangian strain, keeping the entropy constant, are given by

$$\left(\frac{\partial^2 u}{\partial \eta_\alpha^2}\right)_S = v^2 \qquad (3a)$$

$$\left(\frac{\partial^2 U}{\partial \eta_\alpha^2}\right)_S = C_{\alpha\alpha}^S = \rho v^2 \qquad (3b)$$

$$\left(\frac{\partial^2 U_m}{\partial \eta_\alpha^2}\right)_{S_m} = Mv^2 \qquad (3c)$$

where v is the velocity of a sound wave having the strain component η_α (where $\alpha = 1, 2$ and 3 refer to normal strains or stresses for the longitudinal wave and $\alpha = 4$–6 refer to the shear components for the transverse wave) and $C_{\alpha\alpha}^S$ is the second-order isentropic stiffness coefficient.

If the strain occurs under adiabatic conditions, the internal energy of the body increases. Expanding each expressions of the internal energies in powers of the Lagrangean strain η_α at constant entropy about the state of zero strain, and neglecting all terms above the second order, we obtain the elastic internal energies:

$$\Delta u = u(s, \eta_\alpha) - u(s, 0) = \tfrac{1}{2}v^2\eta_\alpha^2 \qquad (4a)$$

$$\Delta U = U(S, \eta_\alpha) - U(S, 0) = \tfrac{1}{2}C_{\alpha\alpha}^S\eta_\alpha^2 = \tfrac{1}{2}\rho v^2\eta_\alpha^2 \qquad (4b)$$

$$\Delta U_m = U_m(S_m, \eta_\alpha) - U_m(S_m, 0) = \tfrac{1}{2}Mv^2\eta_\alpha^2. \qquad (4c)$$

The elastic internal energies taken relative to unit mass, unit volume and unit mole are related to the strain component, η_α, by the material constants v^2, ρv^2 and Mv^2, respectively. Equations (4a)–(4c) hold for the longitudinal velocity, v_l, and the transverse velocity v_t. It should be noted that (4a)–(4c) have different meanings when discussing elastic properties as a function of composition. When the elastic strain is infinitesimal, (4b) is equivalent to the strain energy function [19, 20] in classical elasticity theory.

The elastic internal energy per mole is chosen, if the elastic internal energy is taken relative to unit mass or unit volume; it relates to different amounts of the substances when the composition is changed. Let U_1 and U_2 be the partial molar internal energies of component one (in the present work, B_2O_3) and component two (Bi_2O_3), respectively. Then the mean molar internal energy U_m, can be expressed by

$$U_m = U_1x_1 + U_2x_2 = (U_2 - U_1)x_2 + U_1. \qquad (5)$$

The second-order derivative of (5) with respect to η_α at constant entropy gives

$$Mv^2 = \left(\frac{\partial^2(U_2 - U_1)}{\partial \eta_\alpha^2}\right)_{S_m} x_2 + \left(\frac{\partial^2 U_1}{\partial \eta_\alpha^2}\right)_{S_m} \qquad (6)$$

where x_1 and x_2 are the mol% of the B_2O_3 and Bi_2O_3 respectively. When we plot Mv^2 against x_2, each of

$$\left(\frac{\partial^2 U_1}{\partial \eta_\alpha^2}\right)_{S_m}$$

and

$$\left(\frac{\partial^2 U_2}{\partial \eta_\alpha^2}\right)_{S_m}$$

can be determined in principle from the tangential line of the curve with respect to x_2. If we define the elastic internal energies of component one and two respectively as

$$\Delta U_1 = \frac{1}{2}\left(\frac{\partial^2 U_1}{\partial \eta_\alpha^2}\right)_{S_m}\eta_\alpha^2 \qquad (7)$$

and

$$\Delta U_2 = \frac{1}{2}\left(\frac{\partial^2 U_2}{\partial \eta_\alpha^2}\right)_{S_m}\eta_\alpha^2 \qquad (8)$$

then

$$\left(\frac{\partial^2 U_1}{\partial \eta_\alpha^2}\right)_{S_m}$$

and

$$\left(\frac{\partial^2 U_2}{\partial \eta_\alpha^2}\right)_{S_m}$$

represent, respectively, the elastic internal energies per unit mole of B_2O_3 and Bi_2O_3 generated for a given strain. Hence, they express the elastic resistance of the respective components (B_2O_3 and Bi_2O_3) to the deformation.

Table 1. Composition of Bi_2O_3 (starting composition); density ρ; molar mass M; molar volume V; longitudinal and shear ultrasonic velocities v_l, v_t; elastic moduli, L, G; Poisson's ratio σ; and longitudinal and shear internal elastic energies, Mv_l^2, Mv_t^2 of Bi_2O_3–B_2O_3 glass systems at room temperature.

$Bi_2O_3^*$ (mol%)	ρ (G cm^{-3})	M (G mol^{-1})	V (cm^3)	v_l (km s^{-1})	v_t (km s^{-1})	L (GJ m^{-3})	G (GJ m^{-3})	σ	Mv_l^2 (GJ mol^{-1})	Mv_t^2 (MJ m^{-1})
5	4.224	89.44	20.81	5.783	3.211	141.1	43.5	0.277	2.99	0.92
10	4.483	109.26	23.66	5.951	3.361	158.7	50.6	0.269	3.87	1.22
15	4.704	129.07	26.44	6.182	3.474	179.6	56.6	0.264	4.93	1.56
20	4.912	148.89	29.01	6.307	3.671	195.3	66.2	0.244	5.92	2.00
25	5.201	168.71	30.90	6.211	3.523	200.6	64.6	0.256	6.51	2.09
30	5.361	188.52	32.95	6.105	3.496	199.8	65.5	0.261	7.03	2.30
35	5.691	208.34	34.64	5.893	3.306	197.6	62.2	0.270	7.23	2.28
40	5.796	228.16	36.09	5.603	3.103	187.3	57.4	0.278	7.16	2.20
45	6.211	247.97	37.01	5.302	2.916	174.6	52.8	0.283	6.97	2.11

3. Experimental procedure

3.1. Glass preparation

A series of bismuth–borate glasses were prepared from laboratory reagent grades of Analar boron oxide (B_2O_3, molecular weight 69.622) and Analar bismuth oxide (Bi_2O_3 molecular weight 465.9608), using alumina crucibles (of 100 cm^3 capacity) heated in an electric furnace that was open to the atmosphere. The reagents were mixed and placed in a furnace held at 850 °C for complete fusion. Then, the furnace temperature was raised to 1100 °C and kept for 2 h at this temperature. The glass melts were stirred occasionally with an alumina rod to ensure homogeneous melts. Each melt was case into two mild-steel molds to form glass rods 1 cm long by 1.6 cm diameter. Then, the mold halves were released to prevent cracking, the thin walls of the mold (2 mm) also served to minimize the risk of cracking. After casting, each glass was immediately transferred to an annealing furnace held at 300 °C for 1 h. The furnace was switched off and the glasses were allowed to cool to room temperature at an initial cooling rate of 3 °C min^{-1}. This procedure was employed to prepare glasses with a glass formation range of 5–45 mol% Bi_2O_3 (starting compositions). The compositions of the specimens studied are listed in table 1.

The densities of the glasses were measured by the Archimedes method using toluene as the immersion liquid and they are accurate to ±0.001 g cm^{-3}.

3.2. Ultrasonic measurements

Specimens used for ultrasonic measurements were in the form of cylindrical rods, 1.6 cm diameter of 0.5 cm thick, with end faces optically polished to a parallelism of 1–2 arcsec, using a polishing machine (Metal Research, Multipol 2), with a special jig (MR, MK2) holding the specimen.

The ultrasonic travel time was measured by the pulse echo overlap method [16] at a frequency of 10 MHz and at room temperature.

X-cut and Y-cut quartz transducers were used for the generation and detection of the longitudinal and transverse waves, respectively. The transducer was bonded to the sample with Nonaq stopcock grease $\sim 2.2 \times 10^{-4}$ cm thick and with an acoustic impedance $Z_b = 2.7 \times 10^5$ mech.ohm cm^{-2}.

Table 2. Regression analysis of the variables (density, ρ; longitudinal and shear ultrasonic velocities, v_l, v_t; elastic moduli, L, G; elastic internal energies, Mv_l^2, Mv_t^2 and Poisson's ratio, σ) of the bismuth borate glasses α, β and γ are constants for a quadratic equation, as explained in the text.

Variables I	α	β	γ
ρ	4.01	0.0459	—
SE	0.027	0.0014	—
V_l	5.392	0.0813	−0.001 91
SE	0.094	0.012	0.000 34
V_t	2.924	0.0603	−0.001 378
SE	0.12	0.016	0.000 44
L	109.96	6.3451	−0.1103
SE	5.44	0.71	0.02
G	31.44	2.4584	−0.043 86
SE	4.12	0.54	0.015
σ	0.298	−0.004 14	0.000 095 2
SE	0.013	0.001 74	0.000 048 5
Mv_l^2	1.684	0.2583	−0.002 639
SE	0.21	0.028	0.000 775
Mv_t^2	0.691	0.056 69	−0.001 436
SE	0.097	0.004 98	0.000 843

When the ultrasonic transit time between echoes is measured, it is essential to determine which carrier cycles should properly be compared in observing two echoes. The criterion (known as $n = 0$) proposed by McSkimin [21] and in addition McSkimin and Andreatch [22] has been used to solve this problem [16]. Once a pair of echoes is properly overlapped, the pulse echo overlap technique can measure the absolute transit time within an accuracy of one part in 5000 for round trips greater than 5 μs [16].

3.3. Statistical data analysis

The data was analysed using the statistical package for social sciences (SPSS), by fitting regression curves, and the results are given in table 2. The regression coefficients and their standard errors (SE) are given for the curves shown in figures 1–9. In table 2 $\hat{Y}$ stands for the variables shown in the first column and $\hat{x}$ is the Bi_2O_3 concentration given in mol%. As can be seen in figures 1–9, for most of the variables a curvilinear ($\hat{Y} = \alpha + \beta\hat{x} + \gamma\hat{x}^2$) gives the best fit. However, for the density, the best fit is a straight line ($\hat{Y} = \alpha + \beta\hat{x}$), while the Poisson's ratio is constant ($\hat{Y} = \overline{Y}$).
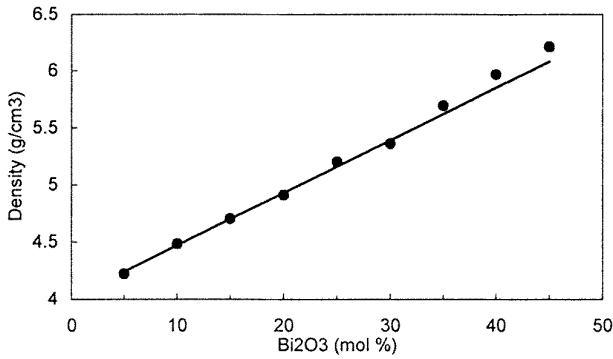
Figure 1. Variation of density with mol% Bi_2O_3 in Bi_2O_3–B_2O_3 glass systems.
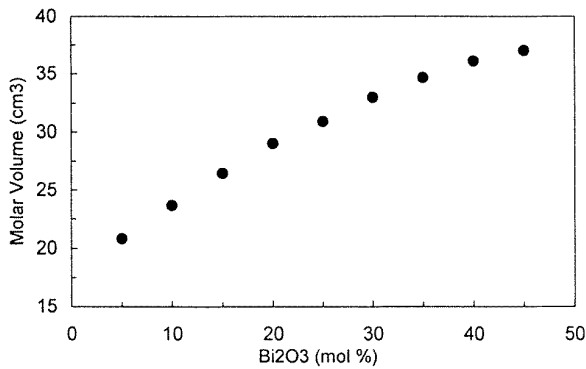
Figure 2. Dependence of molar volume on the composition in Bi_2O_3–B_2O_3 glass systems.
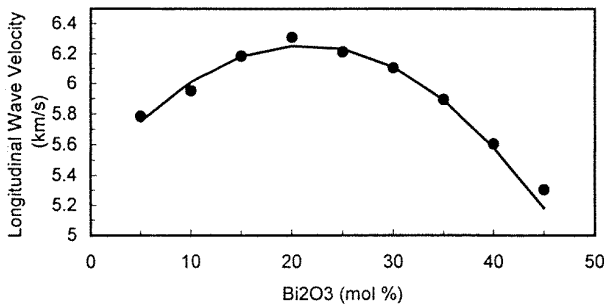
Figure 3. Compositional dependence of the velocity of longitudinal acoustic waves in Bi_2O_3–B_2O_3 glass systems.
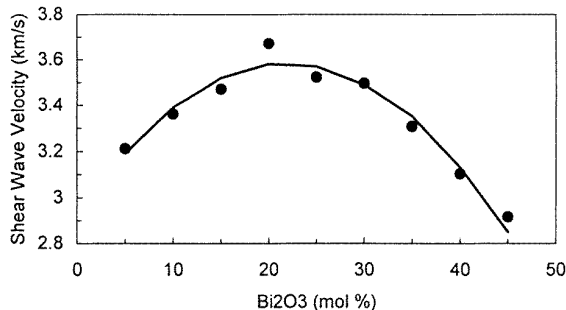
Figure 4. Compositional dependence of the velocity of shear acoustic waves in Bi_2O_3–B_2O_3 glass systems.

4. Results and discussion

Table 1 gives the compositions and the properties of the Bi_2O_3–B_2O_3 glasses. From inspection of this table, it will
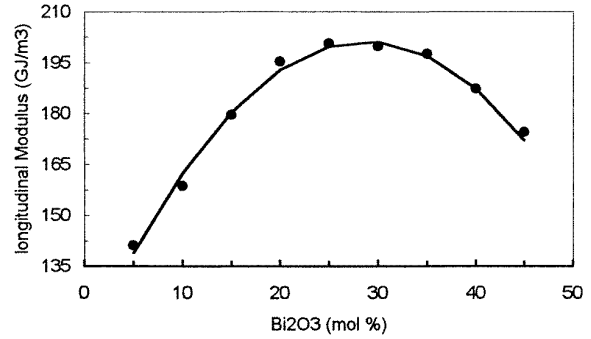
Figure 5. Dependence of longitudinal modulus on the composition of Bi_2O_3–B_2O_3 glass systems.
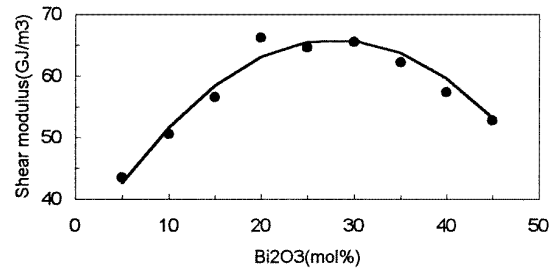
Figure 6. Dependence of the shear modulus on the composition of Bi_2O_3–B_2O_3 glass systems.
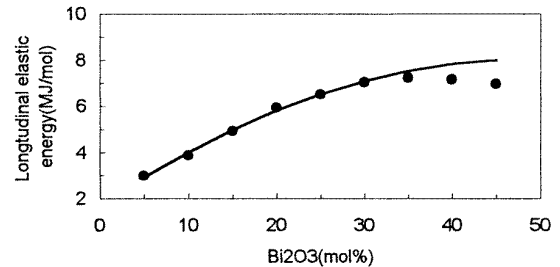
Figure 7. Variation of the longitudinal elastic internal energy with composition of Bi_2O_3–B_2O_3 glass systems.
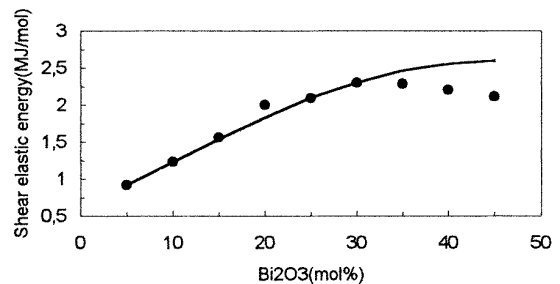
Figure 8. Variation of the shear elastic internal energy with composition of Bi_2O_3–B_2O_3 glass systems.

be observed that there is a change in the behaviour of the compositional dependence of all the properties mentioned so far at a Bi_2O_3 content of approximately 25 mol% (see also figures 1–9).

The variation of the molar volume with the molar per cent of Bi_2O_3 oxide is seen to increase up to 45 mol% Bi_2O_3. The rate of increase is slightly less beyond 25 mol% Bi_2O_3 (see figure 2). The plot of density against mol% (see figure 1)
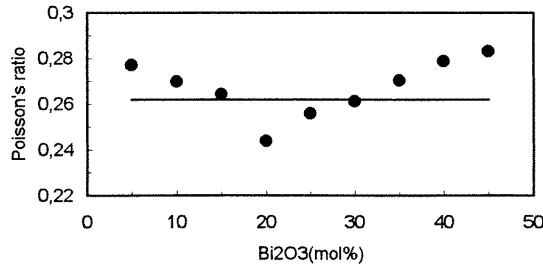
Figure 9. Variation of Poisson's ratio with composition of Bi_2O_3–B_2O_3 glass systems.

showed an increase with increase in mol%, with a point of inflection at about 25 mol%. The increase of the density of the glasses accompanying the addition of Bi_2O_3 is probably attributable to a change in cross-link density and coordination numbers of Bi^{3+} ions.

Figures 3 and 4 show the plots of longitudinal and shear wave velocities v_l^2 and v_t^2 against mol% Bi_2O_3, respectively. Both increase at first with increasing Bi_2O_3 mol% up to a maximum at 25 mol% Bi_2O_3 and then decrease as the Bi_2O_3 mol% increases further. At a given strain, the elastic internal energies of the longitudinal and shear strains per unit mass of the glasses, as functions of composition, follow the tendencies of v_1^2 and v_t^2, respectively.

Figures 5 and 6 show the variations of longitudinal C_{11}^s and shear C_{44}^s moduli against mol% Bi_2O_3. At a given strain, the elastic internal energies of the longitudinal and shear strains per unit volume of the glasses, as functions of composition, follow the tendencies of longitudinal and shear moduli, respectively. Both longitudinal and shear moduli exhibit maxima at different compositions (longitudinal modulus at 25 mol% Bi_2O_3 and shear modulus at 20 mol% Bi_2O_3). This difference arises numerically from the fact that the different magnitudes of v_l^2 and v_t^2 as a function of mol% Bi_2O_3 curves are multiplied by the density, which increases monotonically with increasing Bi_2O_3 composition. One reason for this difference may come from the volume effect, in that C_{44} expresses the resistance of the body to deformation where no change in volume is involved, while C_{11} expresses the resistance where compressions and expansions are involved.

Figures 7 and 8 show the variations of the elastic internal energies of the longitudinal and shear strains per unit mole of the glasses (Mv_l^2 and Mv_t^2), respectively, as functions of the Bi_2O_3 composition. The magnitude of Mv_l^2 and Mv_t^2 show maxima at different Bi_2O_3 compositions (Mv_l^2 at 35 mol% and Mv_t^2 at 30 mol%). This difference arises numerically from the fact that the different magnitudes of the v_l^2 and v_t^2 as functions of Bi_2O_3 compositions curves are multiplied by the molar mass, which increases linearly with increasing Bi_2O_3 composition, this will be explained later.

By applying (6) to figures 7 and 8, the following relations may be obtained for Mv_l^2 and Mv_t^2 as functions of composition:

$$\left(\frac{\partial^2 U_1}{\partial \eta_\alpha^2}\right)_{S_m} < \left(\frac{\partial^2 U_2}{\partial \eta_\alpha^2}\right)_{S_m} \qquad (9)$$

$$\left(\frac{\partial^2 U_1}{\partial \eta_\alpha^2}\right)_{S_m} = \left(\frac{\partial^2 U_2}{\partial \eta_\alpha^2}\right)_{S_m} \qquad (10)$$

$$\left(\frac{\partial^2 U_1}{\partial \eta_\alpha^2}\right)_{S_m} > \left(\frac{\partial^2 U_2}{\partial \eta_\alpha^2}\right)_{S_m} \qquad (11)$$

where (9) is at compositions of less than 35 and 30 mol% Bi_2O_3; (10) is at compositions of 35 and 30 mol% Bi_2O_3; and (11) is at compositions of more than 35 and 30 mol% Bi_2O_3, respectively (see figures 7 and 8).

Equation (9) shows that the network former, B_2O_3, is soft and easily deformed by stress while the modifier, Bi_2O_3, resists deformation more strongly. Except in the vicinity of the maxima (the composition region where boron atoms change from the threefold to the fourfold coordination by addition of modifier Bi_2O_3) the inequality of (9) may therefore arise from the fact that the modifier is enclosed within the network, so that it resists the deformation of the network.

Equation (11) shows that the network former now becomes hard and resists deformation more strongly than the modifier. The composition region corresponding to (11) is in the destruction region, so that the three-dimensional connection of the network has been partly broken up by the formation of non-bridging oxygen ions. B_2O_3 forms into smaller rigid anion groups so that it resists deformation more strongly.

Equation (10) indicates the intermediate state between the two states above, showing that the network former and the modifier equally resist deformation.

The reason why Mv_l^2 and Mv_t^2 exhibit maxima at different compositions can be explained as follows. The partial molar internal energies are regarded as functions of the independent variables S_m, η_α and x (mol% Bi_2O_3), in which η_α are up to quadratic terms. When we consider $[\partial^2 U_1(S_m, \eta_\alpha, x)/\partial \eta_\alpha^2]_{S_m,X}$ and $[\partial^2 U_2(S_m, \eta_\alpha, x)/\partial \eta_\alpha^2]_{S_m,X}$ as functions of x, these depend on each of the strain components. Then, compositions satisfying (10) are generally different between the longitudinal and the shear strain respectively.

By increasing the modifier's composition, B_2O_3 becomes more rigid and the degree to which the modifier prevents the deformation of the surrounding network decreases until, finally, the modifier itself is deformed by the application of stress. These properties depend to an extent on the nature of the strain component.

To interpret our data on the compositional dependence of Poisson's ratio (σ) we first give a general qualitative model of the variation of σ with vitreous composition, developed from an idea expressed by Bridge et al [23], which is summarized as follows. (i) σ decreases with cross-link density (for constant ratio of bending- to stretching-force constant) and (ii) σ decreases with the increasing ratio of bond-bending to stretching force constant F_b/F (at constant cross-link density). If these mechanisms are then applied in our case, we find that the variation of Poisson's ratio with composition should be exactly the reverse of the elastic moduli variation. The experimental data indicate that the Bi^{3+} in octahedral coordination is usually weakly directional—producing a low ratio of F_b/F and correspondingly a high Poisson's ratio in the compositional range of 25–45 mol% Bi_2O_3. In the compositional range of 5–20 mol% Bi_2O_3, σ would fall steeply (see figure 9) where the rate of increase of cross-link density with Bi content is high, as most of the bismuth is in the Bi^{3+} (octahedral) form with its high cross-link density.

5. Conclusion

The elastic properties of the vitreous Bi_2O_3 was measured by ultrasonic pulse echo overlap technique at a frequency of 10 MHz and at room temperature. The obtained conclusions are as follows.

(1) From table 1, one can observe that there is a change in behaviour of the compositional dependence of all the properties measured at around 25 mol% Bi_2O_3.

(2) The density increases with an increase in mol% Bi_2O_3. This is probably attributable to a change in cross-link density, the greater mol wt. of the bismuth atom and the coordination numbers of Bi^{3+} ions.

(3) The longitudinal and shear wave velocities and the elastic moduli of the present glass systems increase with increasing Bi_2O_3 composition, up to 25 mol%, and then decreases as Bi_2O_3 composition increases further.

(4) The variations of the elastic internal energies of longitudinal and shear strains per unit mole of the glasses show that: at compositions less than 35 and 30 mol% Bi_2O_3, the network former B_2O_3 is soft and easily deformed by stress while the modifier Bi_2O_3 resists deformation more strongly. At 35 and 30 mol% Bi_2O_3, the network former and the modifier equally resist deformation. At compositions of more than 35 and 30 mol% Bi_2O_3, the network former becomes hard and resists deformation more strongly than the modifier.

(5) The variation of Poisson's ratio with composition should be exactly the reverse of the elastic moduli variation. It decreases with increasing Bi_2O_3 composition up to 25 mol%, and then increases with increasing Bi_2O_3 composition over 25 mol%.

Acknowledgments

References

[1] Pye L, Frechette V and Kreidl N (eds) 1978 *Borate Glasses* (New York: Plenum)
[2] Thomas S and Parks G 1931 *J. Phys. Chem.* **35** 2091
[3] Zachariasen W 1932 *J. Am. Chem. Soc.* **54** 3841
[4] Warren B, Krutter H and Morningstar O 1936 *J. Am. Ceram. Soc.* **19** 202
[5] Zarzycki S (ed) 1991 *Glasses and Amorphous Materials Science and Technology* vol 9 (Weinheim: VCH)
[6] Atzeni C and Masotti L 1976 *Proc. Int. School of Phys. Enrico Fermi (Course LXIII)* p 499
[7] Osaka A, Ikeda M, Ohbayashi H and Takahashi K 1988 *Yogyokoyokai Shi* **96** 236 (In Japanese)
[8] Kodama M 1985 *J. Phys. Chem. Glasses* **26** 105
[9] Paul A, Singh A and Bhatti S 1990 *Ind. J. Pure Appl. Phys.* **28** 483
[10] Makishima A and Mackenzie J 1973 *J. Non-Cryst. Solids* **12** 35
[11] Fuxi G, Fengying L and Danganaug G 1986 *J. Non-Cryst. Solids* **80** 468
[12] Yawale S, Pakade S and Adgaonkar C 1992 *Acustica* **76** 103
[13] Yawale S, Pakade S and Adgaonkar C 1995 *Acustica* **81** 184
[14] Pakade S, Yawale S and Adgaonkar C 1991 *Int. Science Congress on Ultrasonics (ICU-91)* (New Delhi: NPL)
[15] Nagata K, Ohira K, Yamada H and Goto K 1987 *Metall. Trans.* B **18** 549
[16] Papadakis E 1976 *Physical Acoustics* vol 12, ed W Mason and R Thurton (New York: Academic) pp 277–374
[17] Thurston R 1964 *Physical Acoustics* vol 1, ed W Mason (New York: Academic) pp 1–110
[18] Brugger K 1964 *Phys. Rev.* A **1611** 133
[19] Love A 1927 *A Treatise on the Mathematical Theory of Elasticity* 4th edn (London: Cambridge University Press) (reprinted New York: Dover) pp 98–100
[20] Born M and Huang K 1954 *Dynamical Theory of Crystal Lattices* (London: Clarendon–Oxford University Press) p 135
[21] McSkimin H 1961 *J. Acoust. Soc. Am.* **33** 12
[22] McSkimin H and Andreatch P 1962 *J. Acoust. Soc. Am.* **34** 609
[23] Bridge B, Patel N and Waters D 1983 *Phys. Status Solidi* a **77** 655